FACILE PRODUCTION OF CRYSTALLINE SILVER NANOEMULSION USING AQUEOUS EXTRACTS OF PUTRANJIVA (*DRYPETES ROXBURGII*): SYNTHETIC PROTOCOL OPTIMIZATION THROUGH PRECURSOR, EXTRACT CONCENTRATION AND TEMPERATURE VARIATION STUDY

[1]Basudeb Haldar, [2]Koyel Mallick Haldar

[1]Assistant Professor, [2]Guest Lecturer

[1]Department of Chemistry,

[1]Vivekananda Mahavidyalaya Burdwan, Sripally, Purba Bardhaman, West Bengal, India, Pin – 713103

Abstract : Emulsions of Silver nanoparticles (Ag NPs) were synthesized using a facile, single step, and completely green biosynthetic method employing aqueous leaf and fruit extracts of Putranjiva (*Drypetes roxburgii*) as both the reducing as well as capping agent. The kinetics of nanoparticle formation was also monitored by Ultraviolet–Visible (UV–Vis) spectrophotometric study. Aqueous leaf extract of Putranjiva can reduce silver ions more rapidly than aqueous fruit extract, leading to the formation of highly crystalline nanoemulsion of silver. With varying synthetic conditions like extract concentrations or precursor concentrations, the shape and sizes of the Ag NPs varies. The morphology and crystalline phase of the NPs were determined from High Resolution Transmission Electron Microscopy (HR-TEM), Energy Dispersive X-ray (EDX) analysis, X-ray Diffraction (XRD) analyses. The various phytochemicals present within the Putranjiva plant parts result in effective reduction of silver precursor to nanocrystal. In addition to that, the chemical frameworks of these biogenic molecules are also effective at wrapping around the NPs to provide excellent robustness against agglomeration. Fourier Transform Infra-Red spectroscopic (FTIR) analysis was performed to gather information about the chemical framework. A rigorous study has been performed for procedure optimization by varying different parameters to get most effective stable nanoparticle synthetic protocol.

Index Terms : Silver nanoemulsion, Biogenic synthesis, Putranjiva, Protocol optimization

I. INTRODUCTION

A variety of devices and structures generally ranging from 1 to 100 nm are designated as nanomaterials, those have offered exceptional chemical, optical, magnetic, photoelectrochemical and electronic properties distinctly different from bulk structures (Campbell et.al. 2002, Jain et. al. 2007). The nanoparticles (NP) of noble metals are found to have potential applications in various fields like sensor technology (Nouailhat 2008, Ren et.al. 2005), optical devices (Kamat 2002), catalysis (Liu and Croma 2018), biological labeling (Agasti et.al. 2010), drug delivery system [Liu et.al 2016], and treatment of some cancers (Aslan et. al. 2013, Benelli 2016). Hence, noble metal nanomaterials are at the leading edge of the rapidly developing field of nanotechnology. The sizes, crystal structures, controlled monodispersity and stabilization are the critical factors for specific properties of nanoparticles [Rao et.al. 2002]. Numerous chemical and physical methodologies have been formulated in the recent past, to synthesize noble metal and several other nanostructured materials [Cushing et. al. 2004, Sun et. al. 2002].

An enormously grown interest on this area has led to considerable concern about some of those established synthetic methods. With the development of newer chemical methods, the concern for environmental contaminations is also heightened besides the laborious and expensive chemical procedures those also generate a large amount of hazardous byproducts. This in turn can cause contamination of the nanoparticle surface, leading to adverse effects in medical applications [Shankar et. al. 2004]. On the other hand, physical synthetic methods are problematic due to the enormous consumption of energy required to maintain the high temperature and pressure conditions needed, that restrict the usefulness of these methods too. Thus, a steady need for effective green synthetic protocol has been generated for a clean, environmentally benign but facile method of nanoparticle synthesis.

For green synthesis, the principles include the use of less toxic precursors to prepare nanomaterials; the use of water as a solvent where possible; using the least number of reagents and as few synthetic steps as possible; reducing the amount of by-products and waste; and using a reaction temperature close to room temperature. As a fruitful alternative to the conventional methods, biological methods using sources ranging from unicellular organisms to higher plants fulfill almost all the requisite conditions and are considered safe and ecologically sound for the nanomaterial fabrication [Murphy, 2008]. The contemporary challenge is to find out desired ingredients from efficient biogenic sources and the suitable conditions for tailored nanomaterial synthesis.

Within last two decades, several groups have achieved success in synthesis of noble metal nanoparticles of exotic shapes and morphologies using extracts obtained from various unicellular organisms like bacteria and fungi [Narayanan and Sakthivel 2011, Kalimuthu et.al 2008, Moghaddam et.al. 2015], extracts from biomasses [Vinod et.al 2011, Njagi et.al 2011] as well as extracts of different plant parts [Roy et.al. 2010, Lukman et.al. 2011, Prathna et.al. 2011, Balan et.al. 2016, Bhave et.al. 2018]. From this biogenic synthetic perspective, in the present study, we report on the synthesis of quasi-spherical, and polyhedral or prismatic silver nanostructures using aqueous extract from dried leaf and fruit of Putranjiva at ambient conditions.

Putranjiva (*Drypetes roxburghii*) is a moderate-sized evergreen tree found throughout India. Leaves are simple, shiny dark green, alternate, elliptic-oblong, distantly serrulate and shortly acuminate. Fruits are ellipsoid drupes, seed normally one. The leaves are refrigerant and procreant and are useful in fever, catarrh and sterility. Seeds are sweet, acrid, procreant and refrigerant. It is ophthalmic laxative, aphrodisiac, anti-inflammatory and diuretic, and has been used for many medical applications such as treatment of ulcers of the mouth, stomach, hot swellings, small pox and also useful in burning sensation, ophthalmopathy, hyperdipsia, elephantiasis, constipation, azoospermia, habitual abortion, sterility [Sudharshan et.al. 2009]. It is a potential herbal preservative for peanuts due to its excellent antifungal, insect repellent properties [Tripathi and Kumar 2007]. Fruit pulp contains a large quantity of mannitol, a saponin glucoside and an alkaloid. Kernel contains an essential oil with mustard smell, 2-methyl-butyl iso-thiocyanate yielding glucosides viz. glucoputranjivin, glucojiaputin, glucocochlearin and glucocleomin. Leaves contain β-amyrin and its esters, putrone, putrol, putranjivic acid, methyl putrajivate, stigmasterol and hydrocarbons, triterpene roxburghonic acid and biflavones [Rizk 1987, Krishnamurthi 1969]. The chemical constituents present in the extracts of Putranjiva act as reductants, complexants, and stabilizers (either individually or collectively), which in turn dictate the size and shape of the nanoparticles formed. In our previous report [Haldar et.al. 2013] we synthesized silver nanoparticle from fruit extract of Putranjiva only and reported its mosquoito larvicidal efficacy. In this present article, we present a comparative study of silver nanoparticle synthesis from extracts of putanjiva fruits and leaves. The optimization of synthetic conditions by varying extract concentration and temperature have been performed to get a simple, cost-effective, stable for long time, reproducible protocol of AgNP synthesis.

II. MATERIALS AND METHODS

2.1 Materials

Fresh, mature, green leaves and fruits of *Drypetes roxburgii* were collected from the plants growing within the University of Burdwan campus. Silver nitrate ($AgNO_3$, GR grade) as precursor was procured from Merck, India and used without further purification. Triply distilled de-ionized water was used for the preparation of solutions and extracts. All the experiments were performed in triplicate.

2.2 Methods

2.2.1 Preparation of putranjiva leaf and fruit extracts

The collected leaves and fruits were thoroughly soaked several times in cold water to remove the dust and surface debris and dried by clean tissue paper. The materials were further air dried for two days in closed desiccators, then the leaves were finely cut into small pieces and the fruits were ground into powder using an electrical milling machine. The aqueous extract of both the plant parts were prepared separately by mixing 10 g of the respective material and 200 ml double distilled water taken in Erlenmeyer flasks followed by vigorous shaking with a vortex stirrer (Spinix, India) for an hour. The mixtures were then kept over the vapour of boiling water for 10-15 minutes with intermittent shaking and then filtered by Whatman 41 filterpapers. The final extracts were preserved at 4ºC in Teflon coated container and used within 2 weeks.

2.2.2 Synthesis of silver nanoparticles

A stock solution of 25 mM $AgNO_3$ was prepared and kept in brown glass container in dark. Measured amounts of aqueous silver nitrate solutions mixed with desired concentrations of leaf and fruit extracts of putranjiva separately to yield silver nanoparticle solutions either at room temperature or at elevated temperature to enhance the kinetic rates. For optimization of physico-chemical parameters of the synthetic procedure, the "one factor at a time" method was adopted during synthesis. This design of experiment implied that one experimental factor was varied at a time keeping other factors constant. Applying the method, different sets of solutions were prepared with either varying $AgNO_3$ concentration at fixed plant extract compositions (Table 1) or varying plant extracts at fixed $AgNO_3$ concentrations maintained at finite temperatures (Table 2).

Table 1. The process parameter, plant extract conc. remains fixed but AgNP precursor concentration varies at room temperature (~30ºC).

Leaf Extract Conc. (v/v)	$AgNO_3$ Concentration (mM)				
5%	1.0	2.0	5.0	10.0	20.0
10%	1.0	2.0	5.0	10.0	20.0
20%	1.0	2.0	5.0	10.0	20.0
Fruit Extract Conc. (v/v)	$AgNO_3$ Concentration (mM)				
5%	1.0	2.0	5.0	10.0	20.0
10%	1.0	2.0	5.0	10.0	20.0
20%	1.0	2.0	5.0	10.0	20.0

In one set of experimental solutions, the $AgNO_3$ concentrations were varied between 1 mM to 20 mM at constant leaf and fruit extract concentrations of Putranjiva each separately with 5%, 10% and 20 % (v/v) of the stocks. In another variation of process parameter, the formations of silver nanoparticles were studied at various concentrations of the plant extracts (Leaf and fruit extracts) between 1 - 30% (v/v) maintaining silver nitrate concentration at 2 mM. Each solution was vigorously shaken for 10 minutes on vortex shaker prior UV-Vis study.

Table 2. At fixed precursor concentration, Leaf and Fruit extract concentrations were varied separately at room temperature (~30ºC)

$AgNO_3$ Concentration	Plant Extract Concentration (v/v)				
2 mM	1 %	5 %	10 %	20 %	30 %

2.2.3 Characterization

2.2.3.1 UV-Vis spectroscopy

The bioreduction of Ag precursor ion by ingredients of leaf and fruit were monitored by periodic sampling of the aliquots (100 µl) of the aqueous rection mixtures from time to time. The aliquots were 30 times diluted to 3 ml by deionized water taken in a 10-mm-optical-path-length quartz cuvettee and the absorbance of suspended silver nanoemulsions were recorded on UV–vis spectrophotometer (Shimadzu 2450, Japan) operated at a resolution of 1 nm within 250–850 nm wavelength range. 30 times dilution was made to avoid errors due to high optical density of the solution. Characteristic Surface Plasmon Resonance (SPR) bands of AgNPs confirm the desired synthesis of nanoparticles.

2.2.3.2 HR- TEM & EDX Analysis

Both elemental analysis and morphology of the silver nanoparticles were determined using High-resolution transmission electron microscopy (HR-TEM) and energy dispersive X-ray analysis (EDX) studies. HR-TEM images were taken with a JEOL (JEM-2100) electron microscope operated at an acceleration voltage of 200 kV and beam current of 104.1 µA. The as-formed Ag nanostructures were dried on carbon coated copper grids (300 mesh size) by slow evaporation and then allowed to dry in vacuum at 25ºC for overnight. Selected area electron diffraction (SAED) patterns of the samples were also monitored during the HR-TEM studies. EDX analysis was performed for the same samples by energy dispersive X-ray detector (INCA, Oxford, U.K.) coupled with the HR-TEM instrument.

2.2.3.3 X-ray Diffraction analysis

The purified ultra-centrifuged pellets were freeze dried in vacuum desiccator, and the powdered samples were subjected to X-ray diffraction analysis (Bruker D8 Advance) with a parallel beam optics attachment. The instrument has been operated at a 35 kV voltage and 30 mA current using Ni-filtered Cu Kα radiation (λ = 1.5418 Å) source and the instrument has been calibrated with a standard silicon sample before use.

2.2.3.4 FTIR study

Fourier Transformed Infra-Red (FTIR) analyses were performed to obtain an outlook about the chemical framework around the as-prepared nanoparticles by a FTIR Spectrometer (Perkin Elmer Lx10 – 8873). The individual FTIR spectra of control leaf, fruit extracts alongwith respective AgNP dispersions were monitored to get an idea about the variations in FTIR peaks after nanoparticle formation.

III. RESULTS AND DISCUSSION:

3.1 UV-Vis spectroscopic study

Silver nanoparticles have a characteristics surface plasmon resonance (SPR) absorption band in the UV–Visible region. Thus the reduction of the silver ion to form silver nanoemulsion by the plant leaf or fruit extracts is observable in the UV-vis range 250 to 800 nm. The surface plasmon band arises from the coherent existence of free electrons in the conduction band due to the small particle size [Burda et.al. 2005, Tessier et.al. 2000]. The particle size and their dispersity, chemical surrounding and dielectric constant of the medium may control the width and position of the band maxima as well as the extent of band shift [He et.al 2002, 31, 32]. The aqueous leaf extracts of putranjiva produces nanoparticles which shows a bit wider SPR band (λ_{max} ranging between 430 to 455 nm) whereas the fruit extracts produce rather narrower SPR band having λ_{max} ranging between 407 to 415 nm. Literature suggest that band maxima shifts to red ends for larger average nanoparticle size range [Nalawade et.al. 2014], hence, the observation hints towards less polydispersity as well as smaller average nanoparticle size in favour of the fruit extract. Figure 1(a) shows normalized UV-vis absorption spectra of the 30 times diluted aqueous solutions of the purified pellets of the nanocrystals synthesized with 10% (v/v) of both the plant parts at 2 mM $AgNO_3$ concentration. The redispersed pellets depict two distinct colouration. Yellowish green colouration results from leaf extract whereas the fruit extract develop solution of bright golden yellow. The colour photographs of the solutions are shown in inset of figure 1(a).

3.1.1 Plant extracts concentration variation study

To study the effect of plant extract concentrations on nanoparticle formation, a set of five solutions with leaf extract concentrations 1%, 5%, 10%, 20% and 30% were prepared keeping fixed $AgNO_3$ concentration at 2 mM. The silver nanoparticles start to form rapidly even at room temperature (30ºC ± 1ºC) with increasing concentration of leaf extract. This enhanced rate is expected since higher concentration of leaf must contain greater amount of reducing agents. The absorption spectra of the redispersed pellets of the Ag NP obtained from varying concentrations of leaf extracts are shown in figure 1(b). The figure shows that the absorption spectra for the leaf extract concentrations at 30% and 20% have a significantly broad single absorption bands with λ_{max} at 455 & 445 nm respectively. Interestingly for leaf extract concentrations at 10% or even below, in addition to the SPR band centered at around 420 nm, another broad shoulder band appears which gradually shifts toward longer wavelength with decreasing leaf extract concentration. The shoulder bands observable in these spectra are possibly due to longitudinal plasmon resonance generated from larger sized nanostructures of non-spherical shapes [Sun et.al. 2002]. The rate of colour development is faster (even at room temperature) in case of leaf extract but the overall stabilities of these nanoemulsions are significantly less. This is perhaps due their larger size from greater extent of agglomeration. The suspensions coagulate and settle down within two weeks.

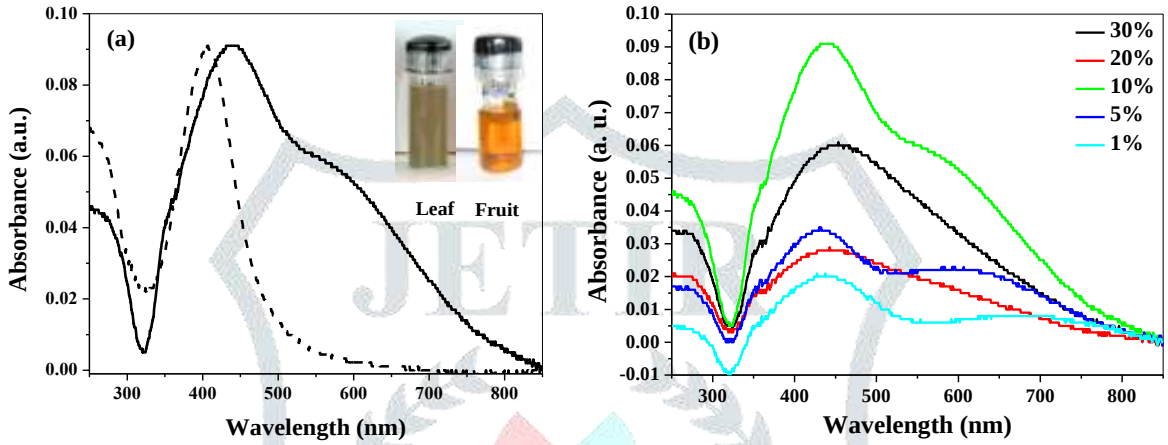

Figure 1: (a) Normalized UV-vis absorption spectra of the dilute aqueous solution of Ag NP synthesized from 10% leaf (—) and fruit extract (----) of Putranjiva at 2 mM $AgNO_3$ concentration. Actual colours of the solutions are shown in inset. (b) SPR absorption spectra at varying leaf extract concentrations at 2 mM $AgNO_3$ concentration.

The variation in fruit extract concentration below 10% (v/v) has no effect on the λ_{max} and shape of the SPR absorption band. A single SPR absorption peak at around 407 nm is observable for all fruit extract concentrations. It implies that the stabilizing effect of fruit extract is greater compared to leaf extract. Additionally, the band position and its width dictate that as-formed silver nanoparticls from fruit extracts are more or less monodispersed and smaller in size range compared to the particles derived from leaf extracts. Another interesting feature is that the rate of colour development for fruit extract is much slow compared to leaf extract. It insisted us to alter the reaction condition by enhancing the reaction temperature. The reaction mixtures with $AgNO_3$ concentration above 5 mM and fruit extract concentration above 10% at elevated temperature produced unstable silver nanoemulsions with large excess of unreacted extract that coagulates and separates out at the bottom of the solution within few hours.

3.1.2 Kinetic study of Ag NP formation at different temperatures

The rate of characteristic colour development might be a qualitative measure of rate of nanoparticle formation. From this parameter it is apparent that leaf extract develops colour faster compared to fruit extract at a finite extract and precursor concentration. On the other hand, in respect of stability and dispersity of the nanoparticles formed, fruit extract becomes a superior choice compared to leaf extract. To amplify the rate of nanoparticle formation from fruit extract, a temperature variation kinetic study was performed at a fixed plant extract and $AgNO_3$ concentration. The kinetics of AgNP generation have been studied for different temperatures at 30ºC, 50ºC, 60ºC and 70ºC with mixtures of 10% fruit extract of the plant and $AgNO_3$ concentration at 2 mM in a thermo-stated water bath. The mixtures turn golden yellow to dark brown after varying finite time depending upon reaction conditions. At the vicinity of completion of NP formation (concluded from rate of variation of absorbance at λmax in UV-Vis study), each nano-colloidal solutions were subjected to centrifuge at 10,000 rpm for 10 minutes. The acquired pellets were redispersed in triple distilled deionized water to get rid of any unreacted biological molecules.

Figure 2 (a), (b) and (c) depicts the variation of absorbance up to a certain range of its value for 2 mM $AgNO_3$ and 10% fruit extract concentration at 30ºC, 50ºC and 70ºC respectively. The figures clearly indicate that at 30ºC the pace of the reaction is extremely slow. The absorbance value of the reaction mixture reaches about 0.085 at λ_{max} in 120 hours i.e. in 5 days whereas, at elevated temperature, the same reaction mixture reaches the same absorbance value within 120 mins i,e. 2 hours. The rate is moderately slow at 50ºC. In this context, it must be mentioned that the nanoemulsion thus formed has a stability issue for enhanced temperature. Though the nanoparticle formation gets pace at increased temperature, but those emulsions are comparatively less stable. The room temperature silver nanoemulsion remains intact for months, but higher temperature product gets settle down after few weeks.

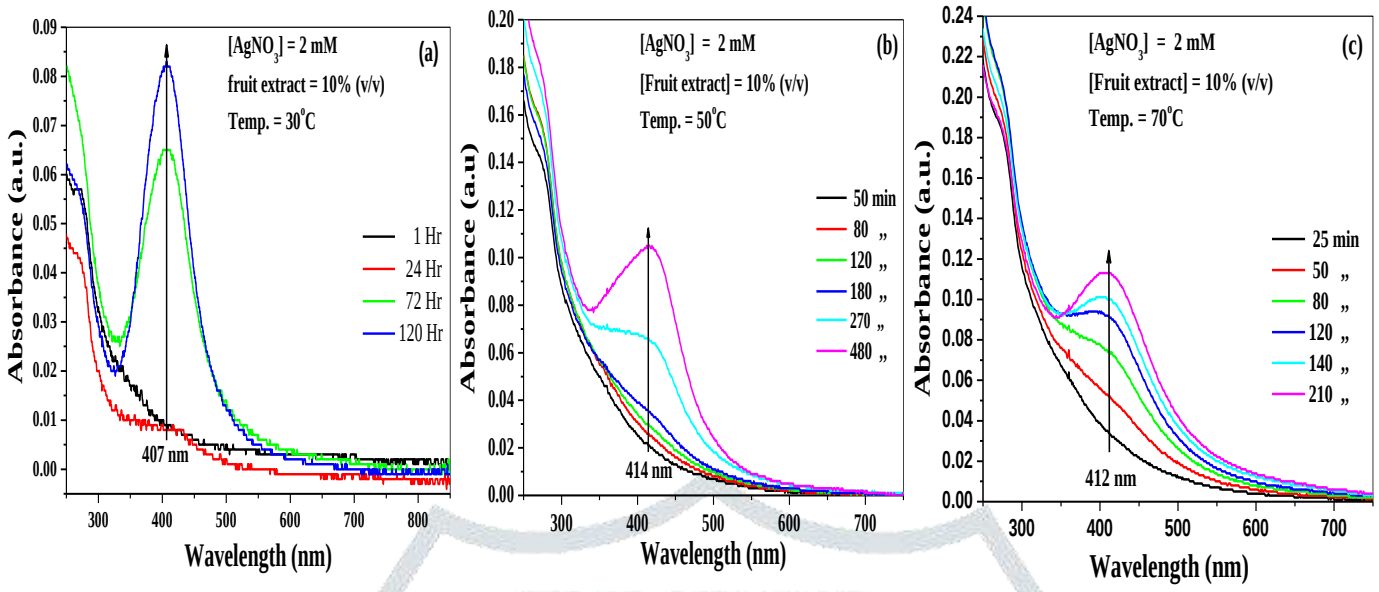

Figure 2: (a) Kinetics of nanoparticle formation for 2 mM $AgNO_3$ and 10% fruit extract concentration at 30ºC. (b) & (c) same composition of reaction mixtures at 50ºC and 70ºC respectively.

3.2 HR- TEM, EDX and Particle size distribution analysis

HR-TEM study was performed to envisage the exact shapes of the particles thus formed as well as to measure the dimensions of the Ag nanocrystals. The study reveals that most of the nano-crystals formed are quasi-spherical (or polyhedral) in shape. It also clearly declares the polydisperse nature of the nanoparticles formed by the ingredients of leaf extract. The HRTEM pictures of nanoparticles formed using fruit extracts establish that the size distribution is really in smaller size range. All these observations are in appropriately accordance with the UV-Vis study.

The energy dispersive X-ray (EDX) spectroscopic analysis was carried out on a random assembly of Ag nanoparticles. Formation of silver crystals was confirmed from the strong signal in the silver region of the EDX spectrum. Metallic silver nanocrystals generally show typical optical absorption peak approximately at 3 keV due to surface plasmon resonance [Magudapatty et al. 2001]. Strong signals for Cu were also observed that have originated from the carbon coated Cu grid.

Figure 3 shows HR-TEM photographs of the as-synthesized Ag NP from leaf extracts of different composition along with their particle size distribution analyses. Figure 3(a) is the HRTEM image with SAED pattern of Ag NPs obtained from 2 mM $AgNO_3$ and 10% leaf extract. It is obvious from the picture that larger-sized crystals are in greater population. The corresponding size distribution pattern is shown in figure 3(b) which describes a wider size distribution having an average size of ~ 60 nm for this particular reaction composition. Similarly, Figure 3(c) and 3(d) demonstrate the HRTEM image and size distribution pattern of Ag NPs obtained from 2 mM $AgNO_3$ and 1% leaf extract. A rather polydisperse but with greater number of smaller particle dimension was observed. Average size reveals at ~ 30 nm. The 1 mM $AgNO_3$ and 5% leaf extract composition yielded a highly polydispered and various shaped nano-crystals (Figure 3e). In addition to quasi-spherical shaped, polyhedral or prismatic shaped and hexagonal shaped crystals are also developed. The largely polydisperse particle population indicate average size of 66 nm (Figure 3f).

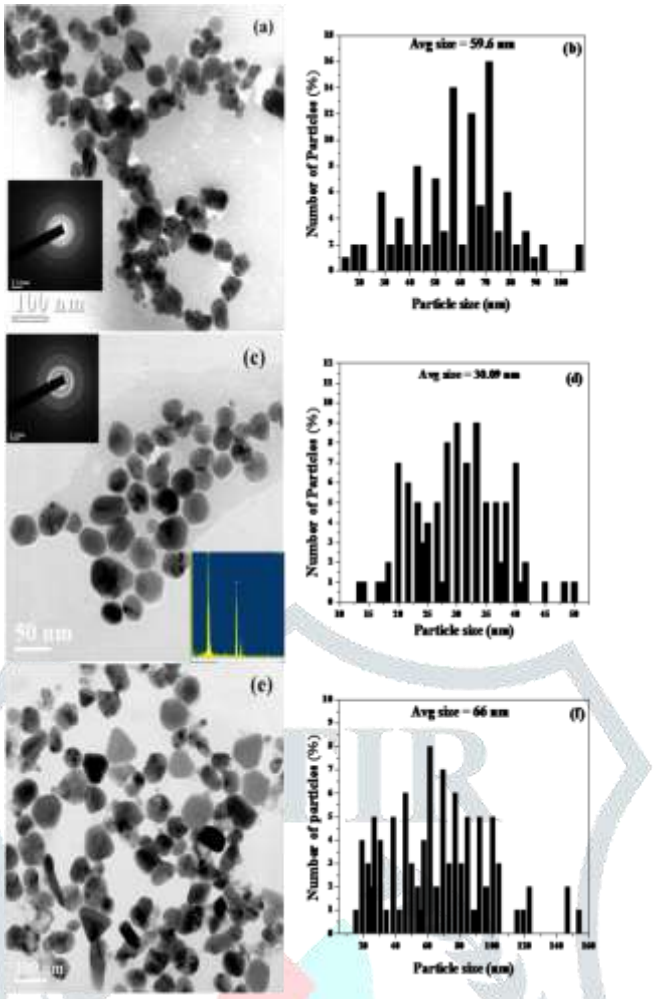

Figure 3: (a) (c) and (e) are HRTEM images of nanocrystals obtained from varying leaf extract concentration and $AgNO_3$ concentration. (b) (d) and (f) are respective size distribution analysis.

HR-TEM photograph of Ag nanocrystals formed at 50°C from 2 mM $AgNO_3$ and 10% fruit extract is shown in Figure 4 (a). A closer view (b) of this image shows the crystal lattice planes with ordered orientation. The lattice fringes are literally visible in one of the particle image. The SAED pattern is included in the inset of figure 4(b) which shows the presence of the (111) plane of the silver. This result from the SAED and HR-TEM analyses is consistent with that of XRD study (discussed later). The particle size distribution (Figure 4c) reveals that majority of particles resides within 10-35 nm range and average particle size is significantly smaller at ~ 26.6 nm.

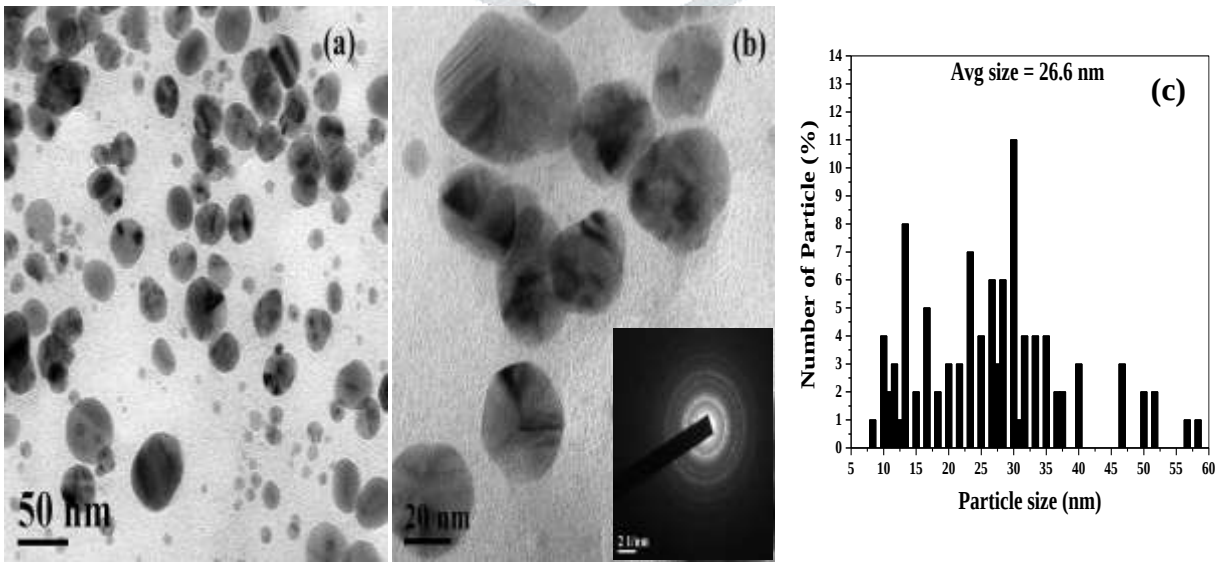

Figure 4: (a) The HRTEM image of AgNP synthesized from 2 mM $AgNO_3$ and 10% fruit extract at 50°C. (b) A closer view and SAED pattern (c) size distribution plot

3.3 X-ray Diffraction analysis

The XRD pattern of as-synthesized nanocrystals is in good agreement with the literature values of fcc crystal structure of silver. Figure 5 (a) shows the XRD pattern observed from the ultra-centrifuged powdered dried pellets obtained from fruit extract. The peaks at respective 2θ values could be assigned to the four different facets known for zero-valent fcc silver representing the 111, 200, 220 and 311 crystal planes due to Bragg's reflections are present. A few unassigned peaks were also noticed in the vicinity of the characteristic peaks. These Bragg peaks might have resulted due to the capping agent stabilizing the nanoparticle. Intense Bragg reflections suggest that strong X-ray scattering centres in the crystalline phase and could be due to capping agents. Independent crystallization of the capping agents was ruled out due to the process of centrifugation and redispersion of the pellet in deionized distilled water after nanoparticle formation as part of purification process. Therefore XRD results also suggest that crystallization of the bio-organic phase occurs on the surface of the silver nanoparticles or vice versa [Shankar et al. 2003a]. Generally, the broadening of peaks in the XRD patterns of solids is attributed to particle size effects [Jenkins and Snyder 1996]. Broader peaks signify smaller particle size and reflect the effects due to experimental conditions on the nucleation and growth of the crystal nuclei [Becheri et al. 2008].

3.4 FT-IR study

A qualitative idea about the functional groups, which are specifically involved for the reduction of the Ag^{+} ions and capping of the silver nanocrystals synthesized from plant broth can be obtained from FT-IR measurements. FT-IR absorption spectra of 10% aqueous fruit extract of Putranjiva as control and the water dispersed pellet of the purified Ag NP from fruit extract are shown in Figure 5(b) which apparently indicates the evidence of chemical bonding between the putranjiva and Ag nanoparticles. In case of control putranjiva fruit extract, several absorbance bands appear at around 3655-3360, 2104, 1594, 1496, 1360 cm^{-1}. For purified nanoparticles of silver the FT-IR spectrum distinctly modifies and the most prominent band appears at 1639 cm^{-1} alongwith the band at 2104 cm^{-1} which become sharper and two wide intense bands at around 580 cm^{-1} and 3500 cm^{-1}. The peaks around 3655-3360 cm^{-1} are indicative of –OH stretching vibrations from different phenolic, 3120 cm^{-1} due to –COOH and at around 2104 cm^{-1} originates from stretching vibration of R–C=CH, –C≡C–, R–N=C=S. The bands at 1594, 1498, 1360 cm^{-1} due to, –C=C– [(in-ring) aromatic], NH_2, –N=O, –C–C– [(in-ring) aromatic]. Moreover, the intense absorption spectra of the nanoparticle at about 1639 cm^{-1} may result from stretching vibration of -C=C- [Huang et al. 2007]. The peak at around 1640 cm-1 is assigned to the amide I bonds of proteins [Shankar et al. 2003b**]**. The bonds or functional groups such as -C-O-C-, –C-O- and -C=C- derived from saponins and the amide I bond derived from the proteins which are present in the fruit extract are possibly the capping ligands of the nanoparticles.

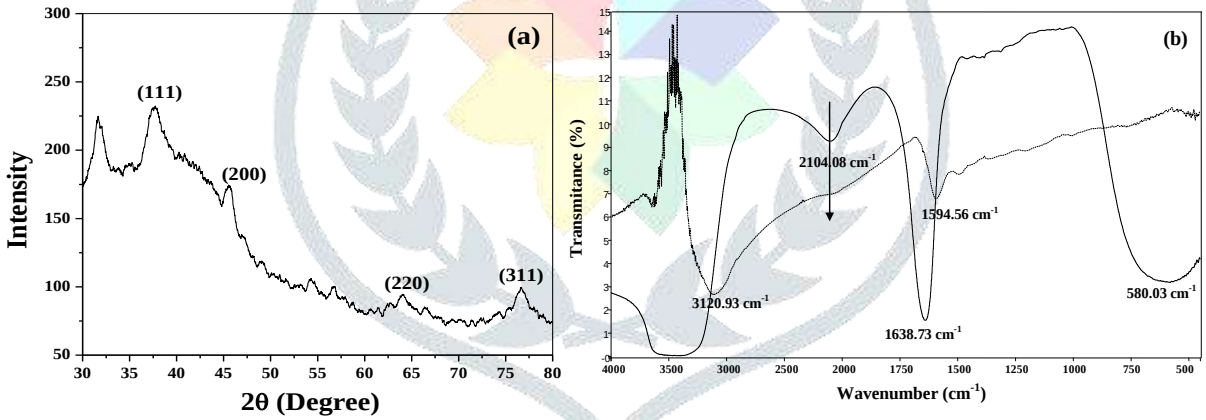

Figure 5: (a) XRD pattern of the biosynthesized silver nanoparticles (b) FTIR spectra of putranjiva fruit extract as control (dotted line) and purified nanoparticle (solid line)

IV. CONCLUSION

The study was conducted to achieve suitable condition of synthesizing stable, monodisperse silver nanocrystals by a green procedure through protocol optimization. The study reveals that low concentration of leaf extracts of putranjiva yields faster but larger and poly-disperse less stable nanoparticles. Varying leaf extract concentration produce a systematic variation in SPR absorption band culminating into less polydisperse but poorly stable, larger nanoparticles at higher leaf extract concentration. Conversely, fruit extract of the same plant can produce comparatively smaller and less polydisperse polyhedral particles, though the kinetics of nanoparticle formation is much slower. Increase in temperature brings pace in formation of nanoparticle of $AgNO_3$-fruit extract system yet too large concentration in fruit extract or too high temperature (above 70°C) reduces the stability of the system drastically. Considering all the process variables, hence, it appears that 10% (v/v) fruit extract, 2mM $AgNO_3$ and about 50°C is an optimum condition for fabrication of appreciably rapid, comparatively stable and less poly-dispersed polyhedral nanocrystals of silver.

V. ACKNOWLEDGEMENT

Financial support from University Grants commission (UGC) is gratefully acknowledged.

REFERENCES:

[1] Agasti, S.S. Rana, S. Park M-H, Kim C. K., You, C-C. Rotello V. M. 2010. Nanoparticles for Detection and Diagnosis, Advanced Drug Delivery Reviews 62(3): 316–328

[2] Moghaddam, A. B. Namvar, F. Moniri, M. Tahir, P. Md. Azizi S. Mohamad R. 2015. Nanoparticles Biosynthesized by Fungi and Yeast: A Review of Their Preparation, Properties, and Medical Applications, Molecules 20, 16540-16565.

[3] Aslan, B. Ozpolat, B. Sood, A. K. and Lopez-Berestein, G. 2013. Nanotechnology in cancer therapy, Journal of Drug Targeting, 21 (10) 904–913.

[4] Balan, K. W. Qing, Y. Wang, X. Liu, T. Palvannan, Y. Wang, F. Ma, Y. Zhang. 2016. Antidiabetic activity of silver nanoparticles from green synthesis using Lonicera japonica leaf extract. RSC Advances. 6:40162–40168.

[5] Becheri, A. Durr, M. Nostro, P.L. Baglioni, P. 2008. Synthesis and characterization of zinc oxide nanoparticles: application to textiles as UV-absorbers Journal of Nanoparticle Research 10 679.

[6] Benelli, G. 2016. Green synthesized nanoparticles in the fight against mosquito-borne Diseases and cancer - a brief review. Enzyme and Microbial Technology, 95, 58-68.

[7] Bhave, A. Dasgupta, S. Hajoori, M. Desai, S. 2018. Nature-friendly synthesis and characterization of silver nanoparticles using leaves extract of Hyptis suaveolens and to evaluate its antibacterial and antioxidant potential, Journal of Emerging Technologies and Innovative Research, 5(7) 870-877.

[8] Burda, C. Chen, X. Narayanan, R. El-Sayed, M.A. 2005. Chemistry and Properties of Nanocrystals of Different Shapes, Chemical Review 105 (4) 1025-1102.

[9] Campbell, C.T. Parker, S.C. Starr, D.E. 2002. The Effect of Size-Dependent Nanoparticle Energetics on Catalyst Sintering. Science, 298, 811-814.

[10] Cushing, B.L. Kolesnichenko, V.L. O'Connor, C.J. 2004. Recent Advances in Liquid-Phase Syntheses of Inorganic Nanoparticles. Chemical Reviews 104 (2) 3893-3946.

[11] Haldar, K.M. Haldar, B. Chandra, G. 2013. Fabrication, characterization and mosquito larvicidal bioassay of silver nanoparticles synthesized from aqueous fruit extract of putranjiva, Drypetes roxburghii (Wall.) Parasitol Res 112, 1451-1459.

[12] He, R. Qian, X. Yin, J. Zhu, Z. 2002. Preparation of polychrome silver nanoparticles in different solvents Journal of Material Chemistry 12, 3783.

[13] Huang, J. Li, Q. Sun, D. Lu, Y. Su, Y. Yang, X. Wang, H. Wang, Y. Shao, W. He, N. Hong, J. Chen, C. 2007. Biosynthesis of silver and gold nanoparticles by novel sundried *Cinnamomum camphora* leaf. Nanotechnology 18: 105104-105114.

[14] Jain, P. K. Huang, X. El-Sayed, I. H. El-Sayed, M. A. 2007. Review of Some Interesting Surface Plasmon Resonance-enhanced Properties of Noble Metal Nanoparticles and Their Applications to Biosystems, Plasmonics 2(3) 107-118.

[15] Jenkins, R. and Snyder, R.L. 1996. Introduction to X-ray powder diffractometry. John Wiley and Sons, New York, pp. 544

[16] Kalimuthu, K. Babu, R.S. Venkataraman, D. Bilal, M. Gurunathan, S. 2008. Biosynthesis of silver nanocrystals by Bacillus licheniformis. Colloids and Surfaces B: Biointerfaces 65, 150-153.

[17] Kamat, P.V. 2002. Photophysical, Photochemical and Photocatalytic Aspects of Metal Nanoparticles, Journal of Physical Chemistry B, 106 (32) 7729-7744.

[18] Krishnamurthi, A. 1969. The wealth of India: a dictionary of Indian raw materials and industrial products. In: A. Krishnamurthi, (Ed.), Raw Materials, vol. VIII. Publication and Information Directorate, CSIR, New Delhi, pp. 325–326.

[19] Liu, D. Yang, F. Xiong, F. Gu, N. 2016. The smart drug delivery system and its clinical potential, Theranostics, 6, (9) 1306–1323.

[20] Liu, L. Corma, A. 2018. Metal Catalysts for Heterogeneous Catalysis: From Single Atoms to Nanoclusters and Nanoparticles, Chemical Reviews, 118 (10), 4981–5079

[21] Lukman, A.I. Gong, B. Marjo, C.E. Roessner, U. Harris, A.T. 2011. Facile synthesis, stabilization, and anti-bacterial performance of discrete Ag nanoparticles using Medicago sativa seed exudates, Journal of Colloid and Interface Science 353, 433-444.

[22] Magudapatty, P. Gangopadhyayrans, P. Panigrahi, B. Nair, K.G.M. Dhara, S. 2001. Electrical transport studies of Ag nanoparticles embedded in glass matrix, Physica B 299**:**142-146

[23] Murphy, C.J. 2008. Sustainability as an emerging design criterion in nanoparticle synthesis and applications. Journal of Material Chemistry 18 (19) 2173-2176.

[24] Nalawade, P. Mukherjee, P. Kapoor, S. 2014. Triethylamine induced synthesis of silver and bimetallic (Ag/Au) nanoparticles in glycerol and their antibacterial study, Journal of Nanostructure Chemistry, 4, 113.

[25] Narayanan, K.B Sakthivel, N. 2011. Green synthesis of biogenic metal nanoparticles by terrestrial and aquatic phototrophic and heterotrophic eukaryotes and biocompatible agents, Advances in Colloid and Interface Science. 169 (2)59-79.

[26] Njagi, E.C. Huang, H. Stafford, L. Genuino, H. Galindo, H.M. Collins, J.B. Hoag, G.E. Suib, S.L. 2011. Biosynthesis of iron and silver nanoparticles at room temperature using aqueous Sorghum bran extracts Langmuir 27 (1) 264-271.

[27] Nouailhat, A. 2008. The Uses of Nanotechnologies in An Introduction to Nanoscience and Nanotechnology, ISTE Ltd, London Ch 6. 107-139.

[28] Prathna, T.C. Chandrasekarana, N. Raichur, A. M., Mukherjee, A. 2011. Biomimetic synthesis of silver nanoparticles by Citrus limon (lemon) aqueous extract and theoretical prediction of particle size Colloids and Surfaces. B: Biointerfaces 82 152-159.

[29] Rao, C.N.R. Kulkarni, G.U. Thomas, P.J. Edwards, P.P. 2002. Size-dependent chemistry: properties of nanocrystals. Chemistry A Europian Journal 8 (1) 28-35.

[30] Ren, X. Meng, X. Chen, D. Tang, F. Jiao, J. 2005. Using silver nanoparticle to enhance current response of biosensor, Journal of Biosensensors and Bioelectronics, 21 (3) 433-437.

[31] Rizk, A.M. 1987. The chemical constituents and economic plants of the Euphorbiaceae. Botanical Journal of the Linnean Society 94 (1-2) 293-326.

[32] Roy, N. Mondal, S. Laskar, R.A. Basu, S. Mandal, D. Begum, N.A. 2010. Biogenic synthesis of Au and Ag nanoparticles by Indian propolis and its constituents, Colloids and Surfaces. B: Biointerfaces 76 (1) 317-325.

[33] Shankar, S. S. Ahmad, A. Parischa, R. Sastry, M. 2003. Bioreduction of chloroaurate ions by geranium leaves and its endophytic fungus yields gold nanoparticles of different shapes. Journal of Material Chemistry 13 1822-1826.

[34] Shankar, S.S. Ahmad, A. Sastry, M. 2003. Geranium leaf assisted biosynthesis of silver nanoparticles. Biotechnology Progress 19: 1627-1631

[35] Shankar, S.S. Rai, A. Ahmad, A. Sastry, M. 2004. Rapid synthesis of Au, Ag, and bimetallic Au core–Ag shell nanoparticles using Neem (Azadirachta indica) leaf broth. Journal of Colloid and Interface Science 275 (2) 496-502.

[36] Sharma, V.K. Yngard, R.A. Lin, Y. 2009. Silver nanoparticles: Green synthesis and their antimicrobial activities. Advances in Colloid and Interface Science 145, 83-96.

[37] Sudharshan, S.J. Chinmaya, A. Valleesha, N.C. Prashith Kekuda, T.R. Rajeshwara, A.N. Murthuza, S. 2009. Central Nervous System (CNS) depressant and analgesic activity of methanolic extract of Drypetes roxburghii wall in experimental animal model. Research Journal of Pharmaceutical Technology, 2 (4) 854-857.

[38] Sun, Y. Gates, B. Mayers, B. Xia, Y. 2002. Crystalline silver nanowires by soft solution processing, Nano Letters 2 (2) 165-168.

[39] Sun, Y. Yin, Y. Mayers, B.T. Herricks, T. Xia, Y. 2002. Uniform silver nanowires synthesis by reducing $AgNO_3$ with ethylene glycol in the presence of seeds and poly (vinyl pyrrolidone), Chemistry of Materials 14 (11) 4736-4745.

[40] Tessier, P.M. Velev, O.D. Kalambur, A.T. Rabolt, J.F. Lenhoff, A.M. Kaler, E.W. 2000. Assembly of gold nanostructured films templated by colloidal crystals and use in surface-enhanced Raman spectroscopy, Journal of American Chemical Society 122 (39) 9554- 9555.

[41] Tripathi, N. N. Kumar, N. 2007. Putranjiva roxburghii oil—A potential herbal preservative for peanuts during storage, Journal of Stored Products Research 43, 435-442.

[42] Vinod, V.T.P. Saravanan, P. Sreedhar, B. Keerthi Devi, D. Sashidhar, R.B. 2011. A facile synt hesis and characterization of Ag, Au and Pt nanoparticles using a natural hydrocolloid gum kondagogu (Cochlospermum gossypium). Colloids and Surfaces. B: Biointerfaces 83 (2) 291-298.